Supporting Information

Li^+-induced Fluorescent Metallogel: a case of ESIPT-CHEF and ICT phenomenon

Manish Kumar Dixit[b] and Mrigendra Dubey [a]*

[a]*Soft Materials Research Laboratory, Discipline of Metallurgy Engineering and Materials Science, Indian Institute of Technology Indore, Khandwa Road, Simrol, Indore 453552, India.*

[b]*Department of Chemistry, Indian Institute of Technology (Banaras Hindu University), Varanasi- 221 005, U.P., India.*

Email: mdubey@iiti.ac.in, mrigendradubey@gmail.com

Table of Contents: **Pages**

Lifetime measurement

The lifetime measurements were made using a time-correlated single photon counting (TCSPC) system from Horiba Yovin (Model: Delta Flex). **1/Li**$^{+}$ ($CHCl_3$/MeOH, 1x10^{-3} M), **1/Na**$^{+}$ ($CHCl_3$/MeOH, 1x10^{-3} M), **2/Li**$^{+}$ ($CHCl_3$: DMSO (4:1) /MeOH, 1x10^{-3} M) and **6/Li**$^{+}$ ($CHCl_3$/MeOH, 1x10^{-3} M) were excited at 363 nm, 323 nm and 370 nm, respectively, using a picosecond diode laser (Model: Delta Diode) and data analysis was performed using EzTime (HORIBA Scientific) decay analysis software. Following equation is used to calculate average lifetime value,

$$\tau_{(av)} = \frac{(\alpha_1.\tau_1) + (\alpha_2.\tau_2) + (\alpha_3.\tau_3)}{(\alpha_1+\alpha_2+\alpha_3)}$$

Where, $\tau_{(av)}$ is average lifetime, τ_1, τ_2, τ_3 are decay components and α_1, α_2, α_3 are respective amplitudes.

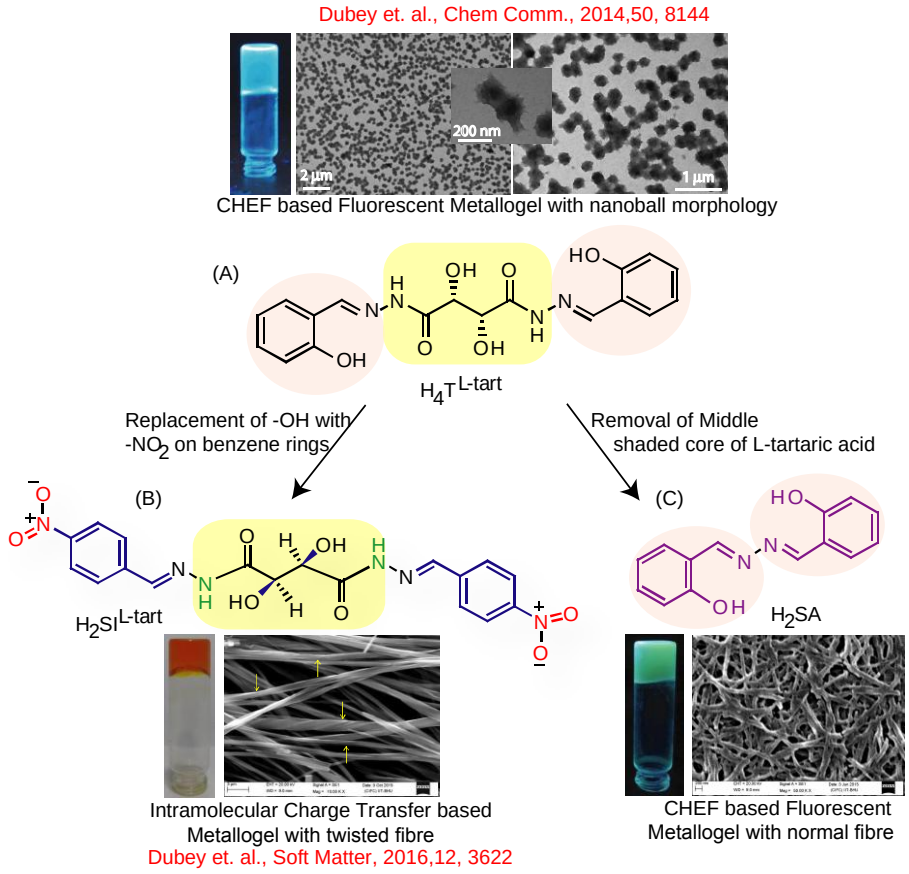

Scheme S1. A schematic presentation of origin of idea towards designing of H_2SA from our previous works. (A) L-tartaric acid derived $H_4T^{L\text{-}tart}$ ligand produces fluorescent metallogel upon LiOH addition and exhibited exceptional nanoball morphology, (B) Modification in $H_4T^{L\text{-}tart}$ produced interesting $H_2SI^{L\text{-}tart}$ ligand which upon LiOH addition turned into an Intramolecular Charge Transfer metallogel with twisted fiber morphology and (C) Removal of middle chiral tartaric core form $H_4T^{L\text{-}tart}$

leads to ligand H_2SA which also produces fluorescent metallogel with long range fibrous morphology.

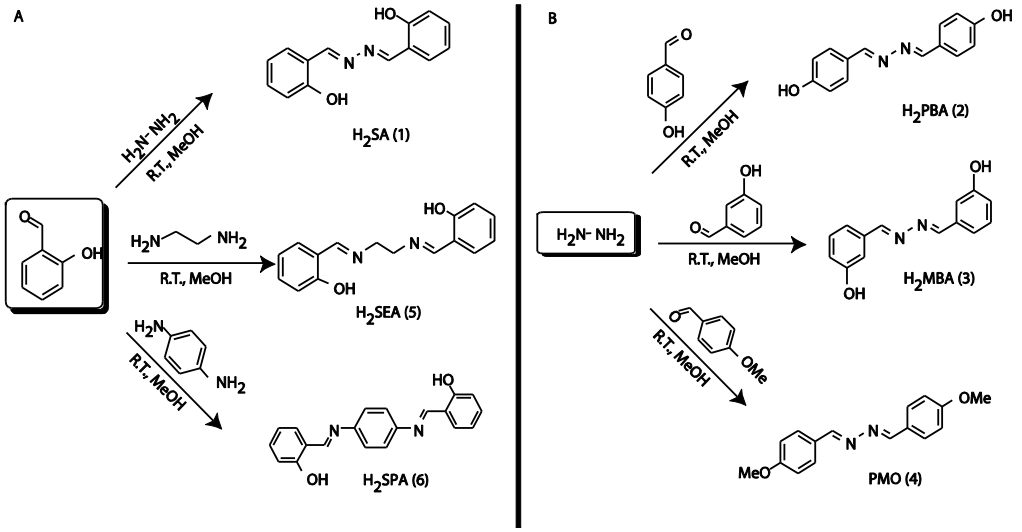

Scheme S2. Synthetic route addopted for the synthesis of compounds (A) **1**, **5, 6** and (B) **2, 3** and **4**.

Table S1: Gelation tests with respect to isomers, LiOH and solvents*

S.N.	Solvent	1+LiOH	2+LiOH	3 +LiOH	4 +LiOH	5 +LiOH	6 +LiOH
1.	Water	S	SP	SP	SP	SP	SP
2.	Acetonitrile	S	S	S	S	S	S
3.	Methanol	S	S	S	S	S	S
4.	Ethanol	S	S	S	S	S	S
5.	DMF	S	S	S	S	S	S
6.	DMSO	S	S	S	S	S	S
7.	Acetone	S	S	S	S	S	S
8.	Chloroform	**G**	SP	S	S	S	SP
9.	DCM	S	SP	S	S	S	SP
10.	THF	S	S	S	S	S	S

*Where, S= solution, G= gel, GP= Gelatinous precipitate, SP= Sparingly soluble

Table S2: Gel or sol formation of **1** with different alkali bases*

Solvent	1+LiOH	1+NaOH	1+KOH	1+CsOH
$CHCl_3$	**G**	GP	S	S

*Where, S= solution, G= gel, GP= Gelatinous precipitate

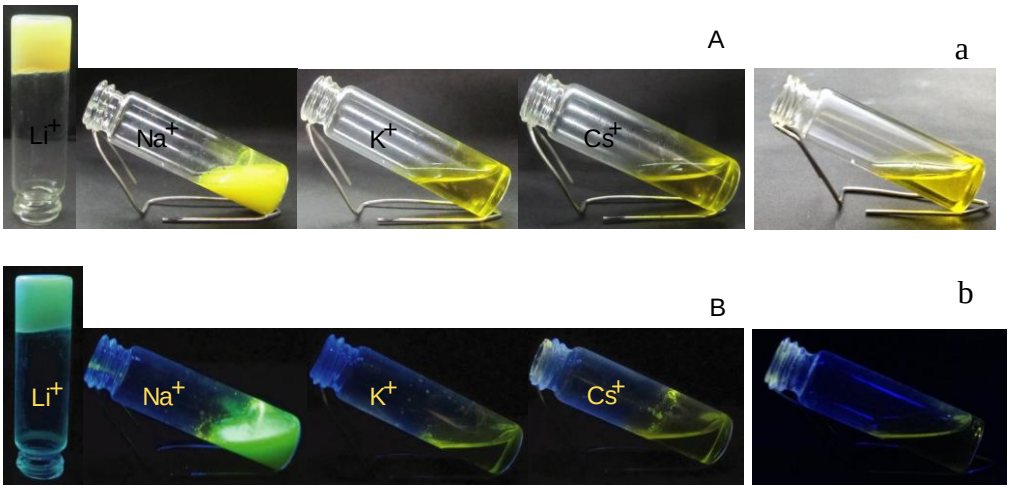

Figure S1. (A) Upper figure represents the gelation property of ligand **1** with Li^+, Na^+, K^+, Cs^+ and (a) TBAOH under nacked eye and **(B)** Lower figure represents similar metallogel and sols under UV light (365 nm).

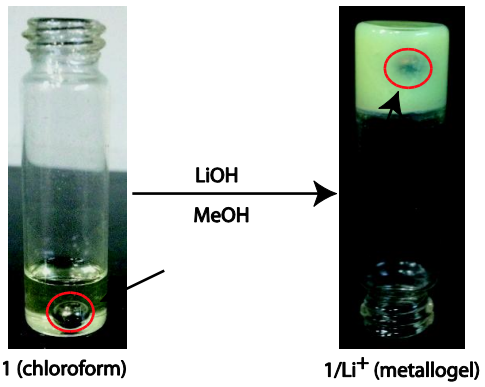

Figure S2. Figure represents the falling ball method using a steel ball (red circled, weight = 8.75gm) in **1** solution which upon gelation does not fall down after vial inversion.

Note: Similar gelation concentration is used for this method *i.e.*, ~$4x10^{-2}$M of **1** (in 0.08 mL $CHCl_3$) and ~$8x10^{-2}$M for LiOH (in 0.02 mL CH_3OH).

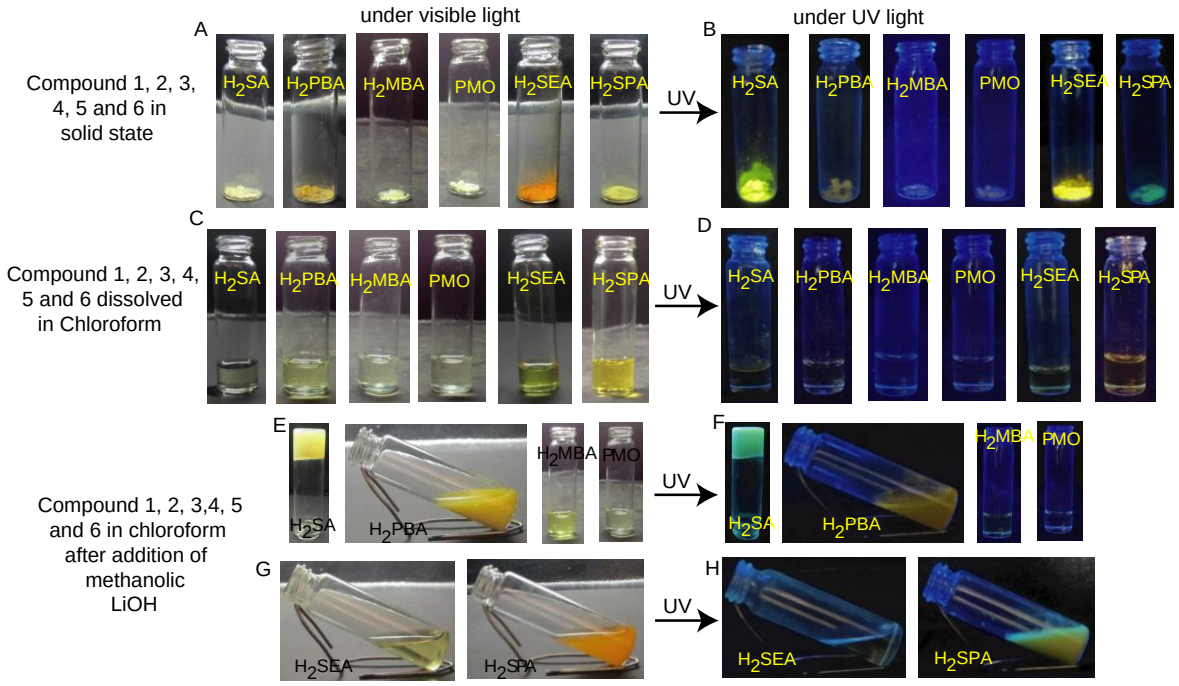

Figure S3. A complete summary of **1**, **2**, **3, 4, 5** and **6** in solid state **(A)** under naked eye and **(B)** under UV light. Solid dissolved in $CHCl_3$ **(C)** under naked eye and **(D)** under UV light. Changes after addition of methanolic LiOH in all above mentioned nonfluorescent solutions under **(E & G)** visible light and **(F & H)** under UV light.

Note: 1, **4**, **5** and **6** were completely soluble in chloroform but **2** and **3** were soluble in chloroform/DMSO (4:1) and chloroform/Methanol (4:1) solvent mixture, respectively.

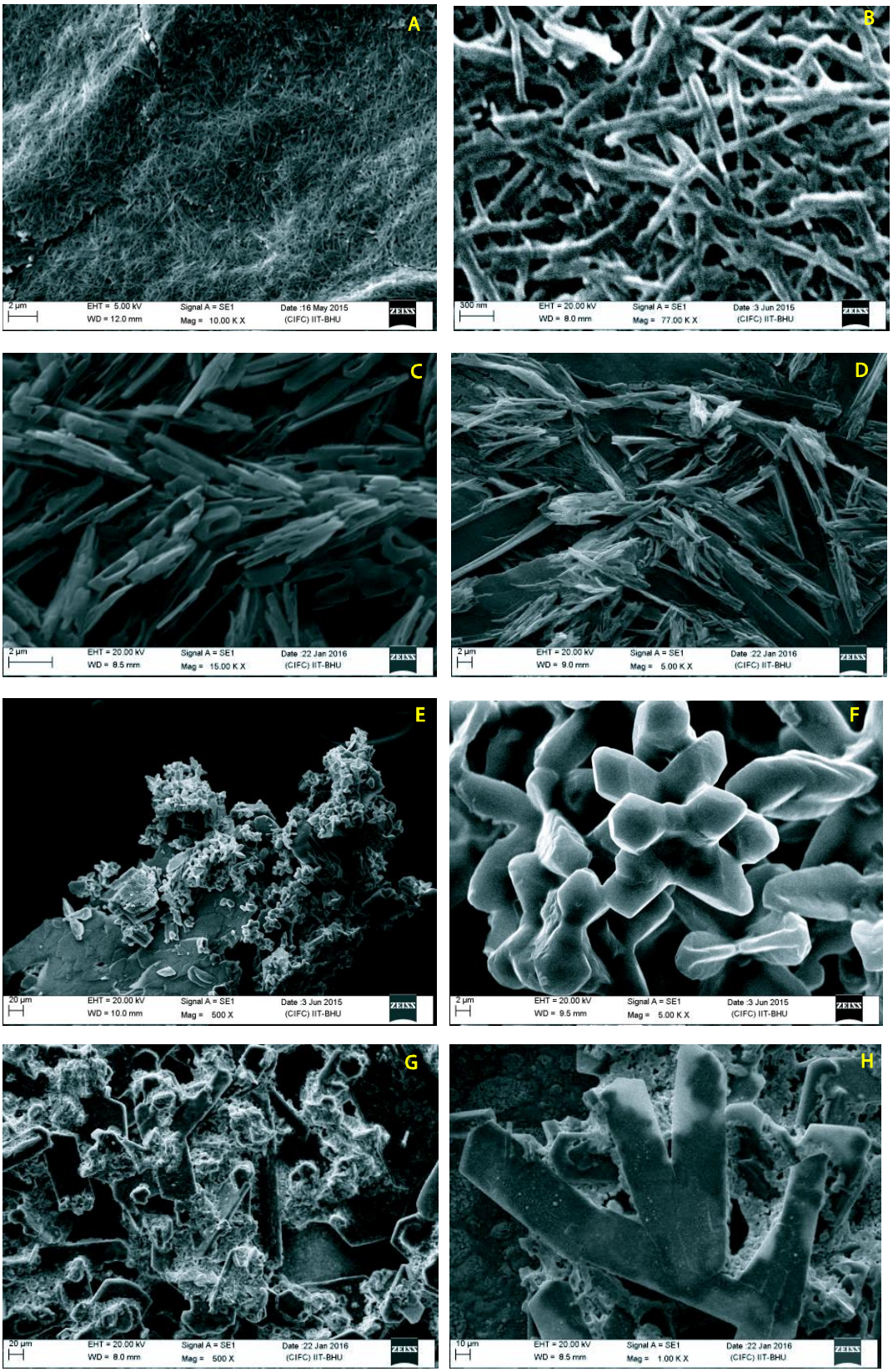

Figure S4. SEM images of **1**/Li^+ dried gel showing (**A and B**) long range fibrous morphology, dried sol of **1**/Na^+ showing (**C and D**) crystalline fibrous nature, dried sol of **1**/K^+ produced (**E and F**) crystals (morphology similar to flower) and dried sol of **1**/Cs^+ produced (**G and H**) normal rod shaped crystals.

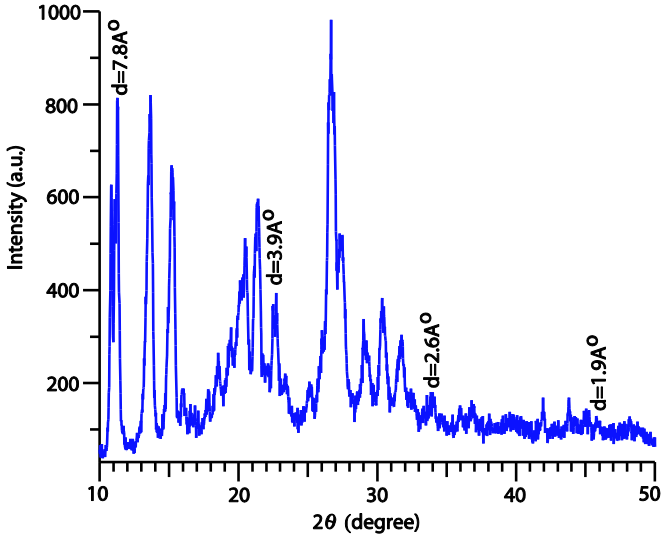

Figure S5. The powder X-ray diffraction pattern of xerogel (1/Li^+) showed several peaks at 2θ values of 10-50 degrees. We found periodic reflections at 2θ = 11.28, 22.52, 33.88 and 45.78, corresponding to d-spacing of 7.83Å, 3.94Å 2.64Å and 1.98Å, respectively were observed. These d-spacing followed a pattern of 1: 1/2: 1/3: 1/4 indicating that the metallogel was organized in a layered pattern, with an inter layer separation of 7.83 Å.

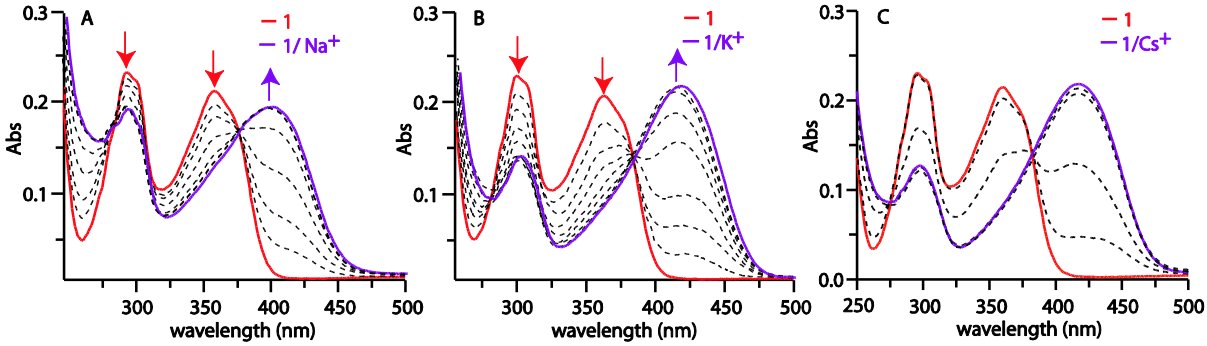

Figure S6. UV-Vis titration of **1** (1x10^{-5}M; $CHCl_3$) with (A) NaOH (1x10^{-3}M; CH_3OH) leads to hypochromic shift at 295 nm and red shift ($\Delta\lambda$=39 nm) of band at 363 nm to 402 nm, (B) KOH (1x10^{-3}M; CH_3OH) again produces hypochromic shift along with blue shift ($\Delta\lambda$=51 nm) to new band at 414 nm at the expense of 363 nm peak and (C) CsOH (1x10^{-3}M; CH_3OH) produces similar effect in which blue shift of 54 nm in band at 363 nm was observed.

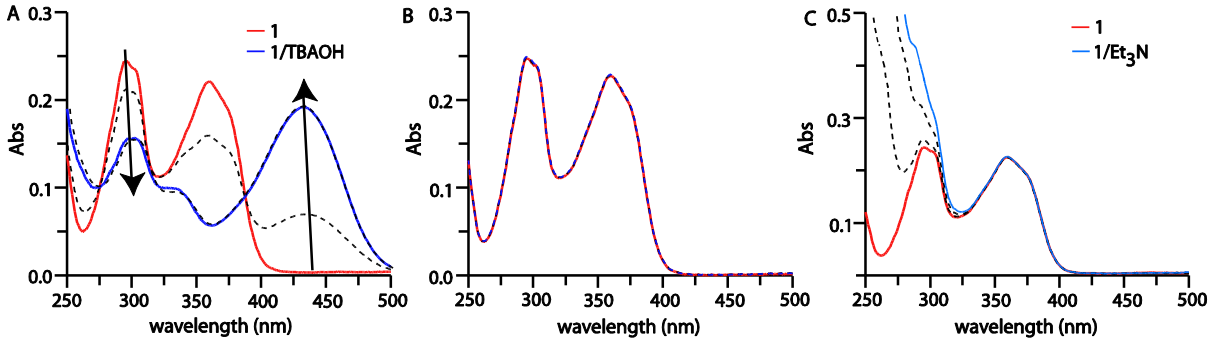

Figure S7. (A) UV-vis spectrum of **1** ($1x10^{-5}$M; ε, 22800 M^{-1} cm^{-1}; $CHCl_3$, red line) with TBAOH ($1x10^{-3}$M; CH_3OH, blue line) undergoes decrease in absorbance of band at 294 nm with slight red shift to 302 nm and peak at 363 nm converts in to new absorption band at 433 nm ($\Delta\lambda$= 70 nm) with a hump at around 334 nm, (B) and (C) treatment of NH_3 and Et_3N to **1** do not produce any significant change.

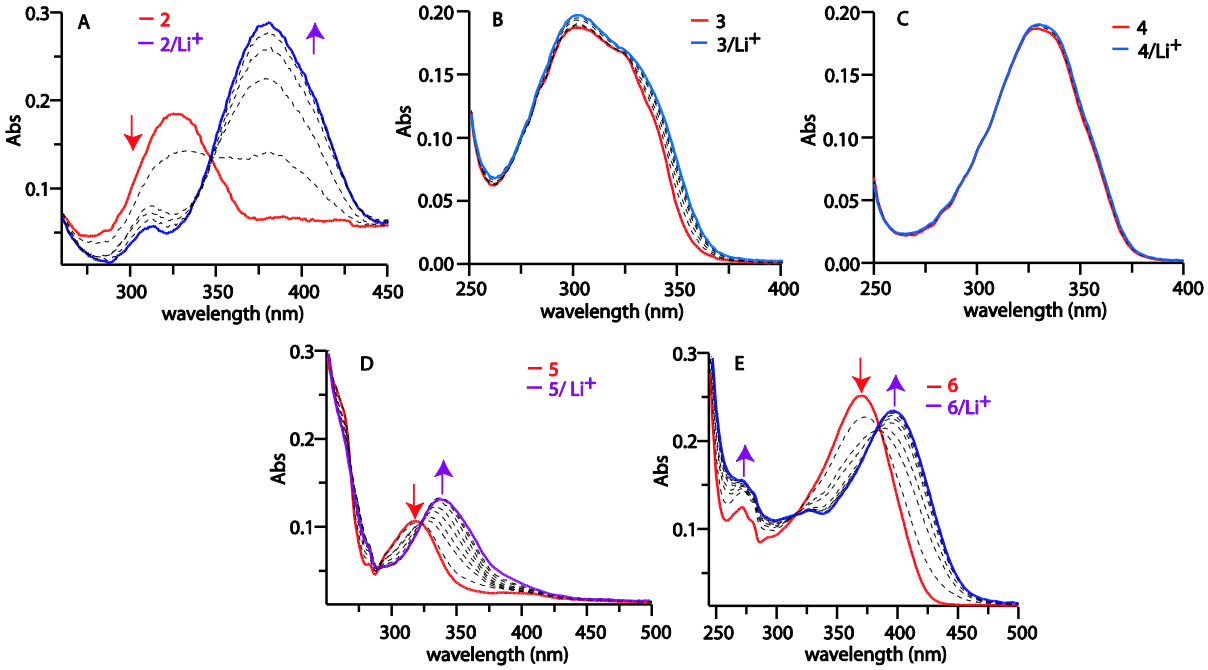

Figure S8. (A) **2** ($1x10^{-5}$ M; ε, 18500 $M^{-1}cm^{-1}$; $CHCl_3$/DMSO, 4:1) upon addition of LiOH ($1x10^{-3}$M; CH_3OH) demonstrates the red shift to 380 nm ($\Delta\lambda$=57 nm) with an isosbestic point at 348 nm, (B) Structural isomer **3** appeared at 303 nm ($1x10^{-5}$ M; ε, 18300 $M^{-1}cm^{-1}$; $CHCl_3$/MeOH, 4:1), (C) compound **4** ($1x10^{-5}$ M; ε, 19500 $M^{-1}cm^{-1}$, $CHCl_3$) at 330 nm do not show any siginificant change after addition of LiOH ($1x10^{-3}$M; CH_3OH), (D) **5** ($1x10^{-5}$M; ε, 10500 $M^{-1}cm^{-1}$; $CHCl_3$) appears at 319 nm which upon LiOH ($1x10^{-3}$M; CH_3OH) addition shifted to 337 nm (ε, 13300 $M^{-1}cm^{-1}$; $CHCl_3$) through an isosbestic point and (E) **6** showed peak at 370 nm ($1x10^{-5}$M; ε, 25000 $M^{-1}cm^{-1}$; $CHCl_3$) in presence of LiOH ($1x10^{-3}$ M, CH_3OH) red shifted to 397 nm with an isosbestic point.

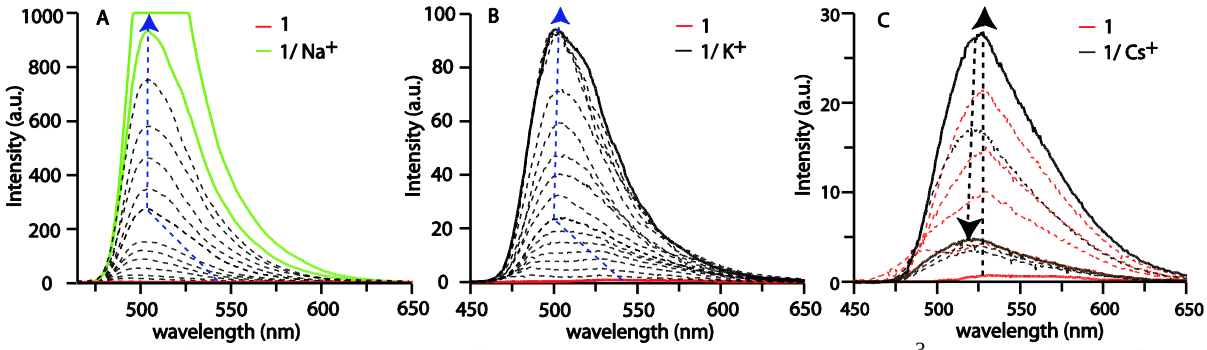

Figure S9: Fluorescence titration between **1** (λ_{ex}= 363 nm, 1x10^{-3} M, $CHCl_3$) and (A) NaOH (10^{-1}M, MeOH), (B) KOH (10^{-1}M, MeOH) and (C) CsOH (10^{-1}M, MeOH) demonstrates the fluorescence intesity is inversly proportional to cation size.

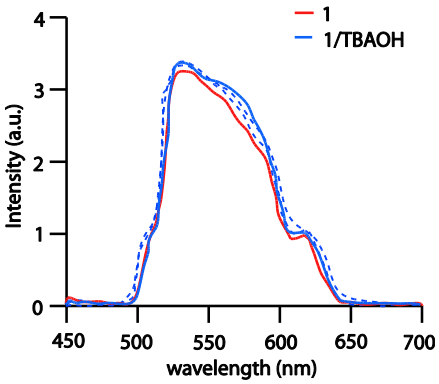

Figure S10: TBAOH (10^{-1}M; MeOH) addition to **1** (10^{-3} M; $CHCl_3$) remain unchanged fluorescence spectral properties.

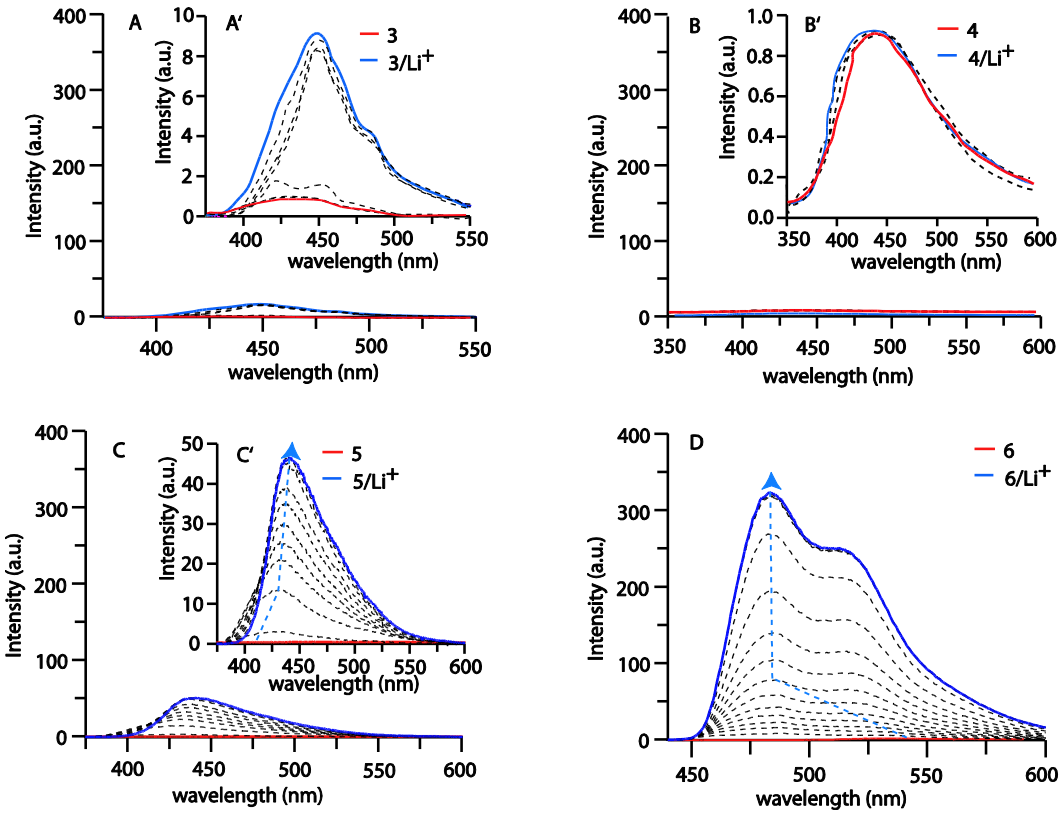

Figure S11: Fluorescence spectrum of **(A)** and **(A') 3** (red line) after LiOH addition (blue line), similarly, **(B)** and **(B') 4** (λ_{ex} = 330nm, 10^{-3}M; $CHCl_3$) remains non fluorescent with LiOH. **(C)** and **(C')** non emmisive **5** (λ_{ex} = 319 nm, 10^{-3}M; $CHCl_3$) displayed a peak at 410 nm (stokes shift= 85500 cm^{-1}) which upon gradual addition of LiOH (10^{-1}M; MeOH) obained a red shift with minor enhancment in fluorescent intensity at 436nm, **(D)** non emmisive **6** (λ_{ex} = 370nm, 10^{-3}M; $CHCl_3$) at 435 nm (stokes shift= 85500cm^{-1}) displays hypsochromic blue shift ($\Delta\lambda$=45nm) upon addition of LiOH (10^{-1}M; MeOH).

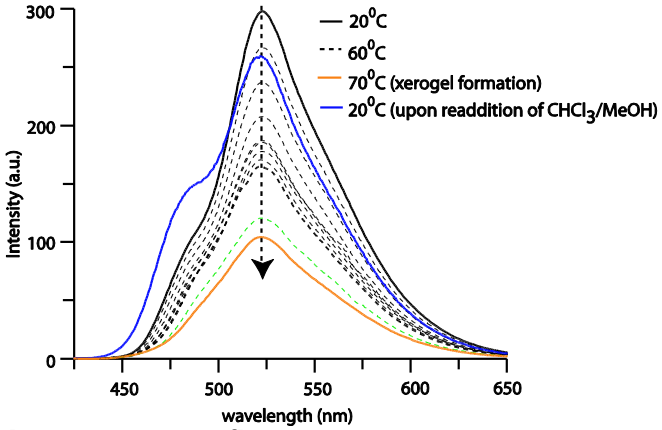

Figure S12: Variable temperature fluorescent experiment (20°C- 70°C) over freshly prepared gel (λ_{ex}= 363nm, ~10^{-2}M) shows quenching of the fluorescence (red line, 70°C) and 90% recovery (blue line) of intensity upon addition of requisite amount of solvent.

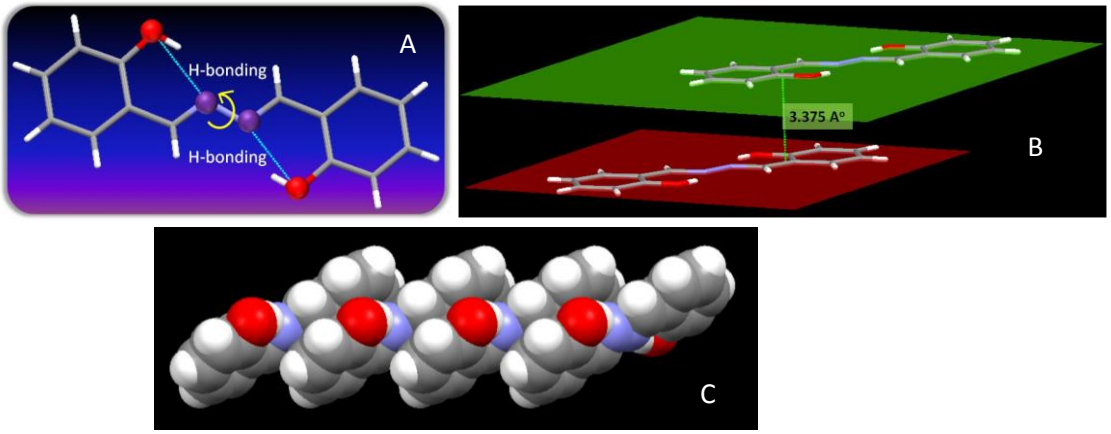

Figure S13: (A) Capped sticks model of crystal **1 (**obtained from 1/CsOH solution**)** demonstrate the H-bonding (2.612 A^o), possibility of ESIPT phenomenon and rotation around N9-N9 bond, (B) Distance between planar surfaces of two molecules was accounted as 3.375 A^o which falls in appropriate range of π–π stacking and (C) Crystal packing (spacefill model) shows possibility of π–π stacking which is in full agreement with the results obtained from dilution of gel in fluorescence experiment and Space fill model of crystal $1/Cs^+$.

Note: Crystallographic data and refinement parameters for **1** (obtained from 1/CsOH solution)**:** Empirical formula $C_{14}H_{12}N_2O_2$**,** Formula weight 120.13, Colour Yellow, Crystal size/mm 0.66 ≤ 0.51 ≤ 0.61, Crystal system Monoclinic, Space group $P2_1/n$, Unit cell dimensions a = 8.5166 (6) Å, α = 90 °; b = 6.3092 (4) Å, β = 107.898° (7); c = 11.8280 (8) Å, γ = 90°, Volume (Å^3) 604.80 (7), Z 4, Density (calc., Mg m^{-3}) 1.3303, Absorption coefficient (mm^{-1}) 0.090, F (000) 256.1, HyPix3000 Diffractometer, Temperature (K) 293(2), μ(Mo Kα) = 0.091 mm^{-1}, θ range (°) for data collection 3.52–26.81, Limiting indices -10 ≤h ≤ 10; -8 ≤ k≤ 7; -14 ≤ l ≤ 15, Reflections collected 4207, Independent reflections 1278 [R_{int} = 0.0970, R_{sigma} = 0.0536], Data/restraints/parameters 1278/0/86, Goodness-of-fit on F^2 1.026, Final R indexes [I>=2σ(I)] R_1 = 0.0691, wR_2 = 0.1974, Final R indexes (all data) R_1 = 0.0787, wR_2 = 0.2112, Largest diff. peak/hole / e Å^{-3} 0.23/-0.36, CCDC 1827279.

H bonds: N9…H7 2.612 A°

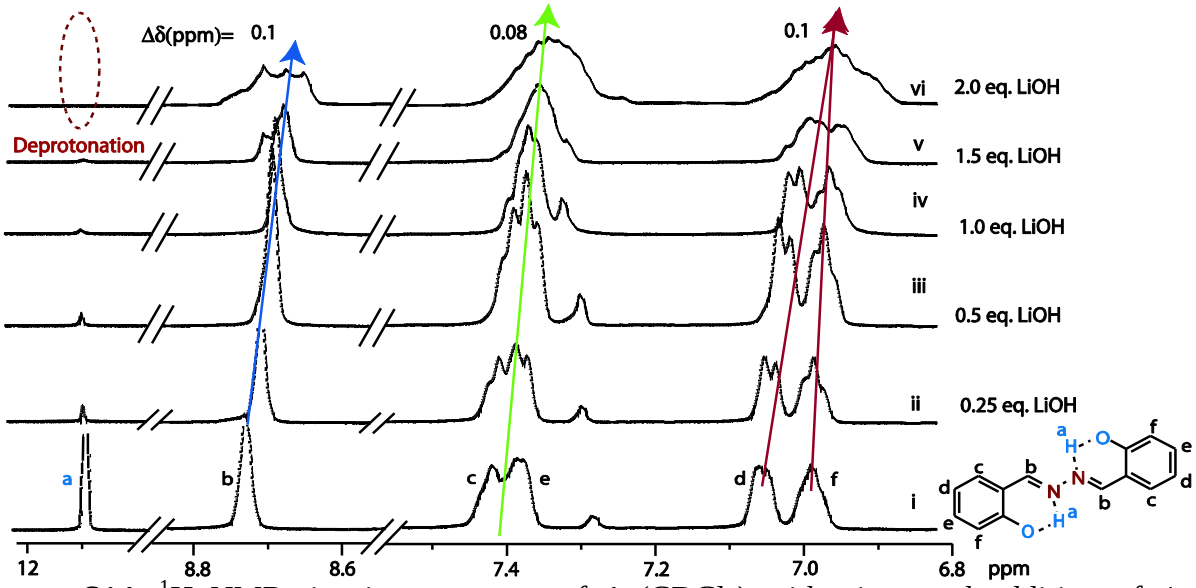

Figure S14. ^{1}H NMR titration spectrum of **1** ($CDCl_3$) with piecemeal addition of 4 equivalents of LiOH (CD_3OD). Chemical structure of **1** along with alphabetic assignment of protons and its corresponding peak shown in spectrum.

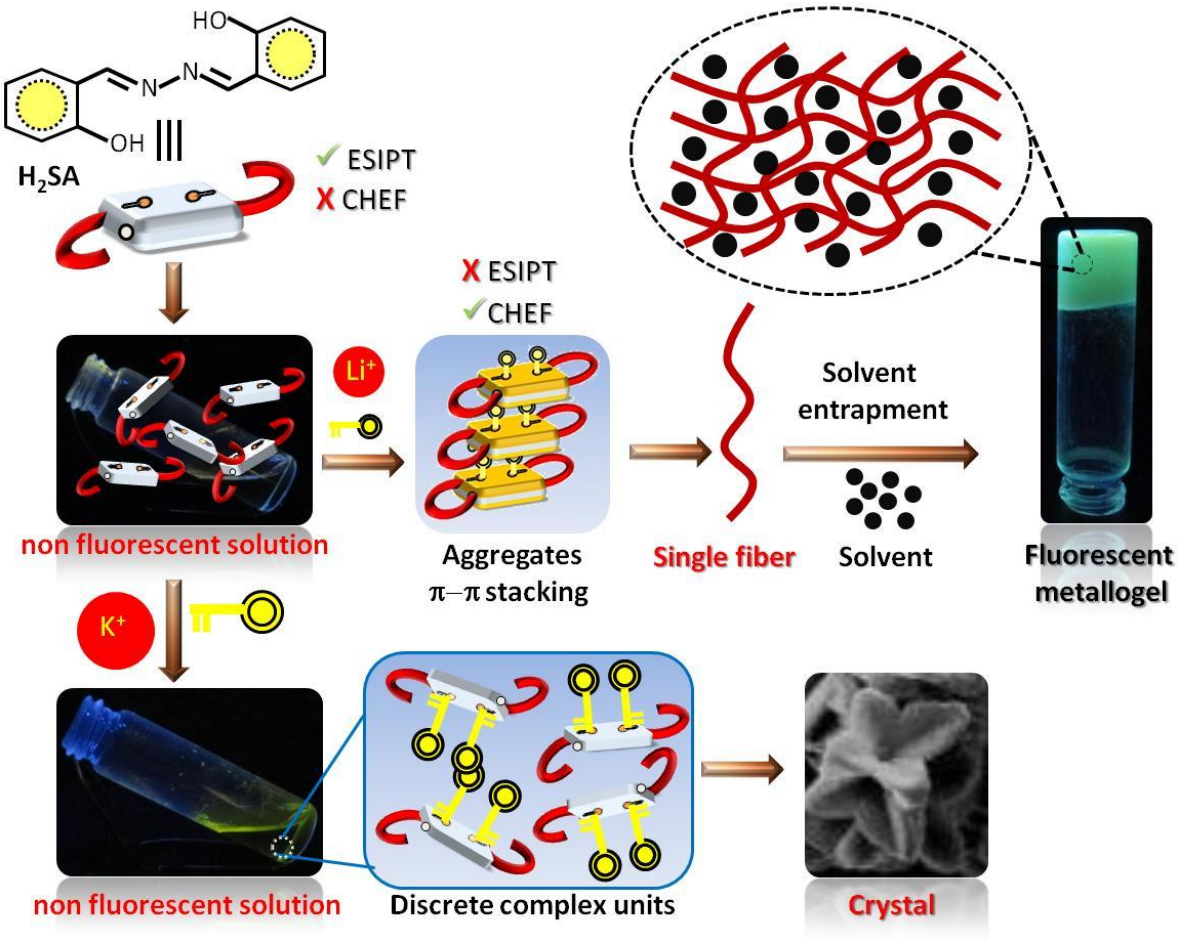

Figure S15: A diagrammatic presentation of plausible mechanism behind metallogel formation.